Строительные материалы и изделия
Construction Materials and Products

journal homepage: https://bstu-journals.ru

ISSN
2618-7183

DOI: 10.58224/2618-7183-2025-8-4-3

Effects of multi-walled carbon nanotubes on polymer degradation in modified binder and their impact on the performance of stone mastic asphalt concrete

Obukhova S.Yu.* [1], **Gladkikh V.A.** [1], **Kuzmina T.K.** [1]

[1] National Research Moscow State University of Civil Engineering, Russia

Abstract. Bitumen, the primary binder in asphalt concrete, lacks sufficient resistance to prolonged mechanical and environmental stress. To improve its durability, styrene-butadiene polymers are commonly used, although they are prone to oxidative degradation and phase instability. This study proposes a nanostructured approach to enhancing the stability and performance of polymer-modified bitumen (PMB) through the synergistic use of multiwalled carbon nanotubes (MWCNTs) and hydrocarbon plasticizers-specifically, selective oil refining extracts (SORE) and vacuum distillates (VD). Short-term oxidative degradation was assessed using isothermal RTFOT aging at 153, 163, and 173 °C. A classical first-order Arrhenius kinetic model was applied, with dynamic viscosity serving as a rheological proxy for SBS network integrity. Nanomodified compositions exhibited a 6-7-fold reduction in degradation rate constant (from 13.97×10^{-5} to 1.98×10^{-5} s^{-1}) and a 25-60% decrease in the preexponential factor, indicating suppressed molecular mobility and enhanced network cohesion. Performance was validated on SMA-16 specimens, showing up to 240% improvement in shear adhesion at 50 °C and 27% higher water resistance. Rutting resistance also increased, with rut depth reduced to 1.6–1.8 mm after 20,000 loading cycles. To integrate physical, mechanical, and durability characteristics, a set of Partial Quality Criteria (PQC) was developed and used to calculate a Generalized Effectiveness Coefficient (GEC), supporting multi-criteria optimization of asphalt mixtures. These findings confirm that nanostructured dispersed systems based on MWCNTs and hydrocarbon carriers not only delay oxidative degradation but also ensure multifunctional performance gains critical for high-traffic pavement applications.

Keywords: multi-walled carbon nanotubes, polymer-modified binder, oxidative aging, Arrhenius kinetics; activation energy, stone mastic asphalt concrete, performance characteristics, tensile strength ratio, shear stability, resistance to rutting by rolling a loaded wheel

*Corresponding author E-mail: shehovtsovasyu@mgsu.ru

Received June 3, 2025; Received in revised form July 18, 2025; Accepted August 22, 2025

Please cite this article as: Obukhova S.Yu., Gladkikh V.A., Kuzmina T.K. Effects of multi-walled carbon nanotubes on polymer degradation in modified binder and their impact on the performance of stone mastic asphalt concrete. Construction Materials and Products. 2025. 8 (4). 3. DOI: 10.58224/2618-7183-2025-8-4-3

1. INTRODUCTION

Asphalt concrete is the most widely used material for road pavement construction in industrialized countries, including the Russian Federation [1]. Asphalt concrete pavements are applied on roads with varying traffic loads. This primary structural road-building material consists of mineral aggregates (crushed stone, crushed sand, mineral powder) and an organic binder (bitumen) [2]. Due to the presence of an organic binder, asphalt concrete is sensitive to ambient temperature fluctuations. In combination with the aging processes in the bitumen binder and mechanical stresses from traffic, this sensitivity causes insufficient operational reliability under fluctuating temperatures, leading to cracking, plastic deformation, premature wear, and further material degradation [3, 4]. The structure of asphalt concrete, comprising a mineral skeleton and bitumen matrix, endows it with a specific set of properties that depend on usage conditions. Its physical and mechanical properties vary with structural parameters, which differ according to the concentration of the organic binder and the particle size distribution of the mineral components [5].

For roads with high traffic loads, the use of stone mastic asphalt (SMA) is preferred due to its denser structure. The properties of SMA largely depend on the characteristics of the bituminous binder, which bonds the mineral components and ensures pavement durability and stability [6]. Key influences of the bitumen binder on SMA include strength, deformation resistance, crack resistance, and durability. The binder must ensure reliable adhesion under varying temperatures. However, ordinary bitumen's temperature sensitivity and aging from oxidation and ultraviolet (UV) exposure negatively impact asphalt's lifespan [7].

Various additives address these issues [8]. Polymer-modified bitumen is frequently used in SMA, expanding the stable temperature range to reduce risks of cracking in cold weather and rutting in heat, although the delamination and aging of polymer–bitumen binders remain challenges [9]. Adding fibers improves cohesion and adhesion between bitumen and the aggregate [10]; however, uniform distribution is challenging, sometimes worsening asphalt's mechanical properties due to clumping [11]. Nanomaterials offer promising enhancements due to unique properties like high surface area, mechanical strength, and thermal stability, making them ideal for improving bituminous binders and asphalt. Nanomaterials such as graphene, carbon fibers, nanotubes, and nanoparticles have demonstrated effectiveness [12]. Studies show nanoclay enhances tensile strength and aging resistance in asphalt, while combining titanium dioxide with styrene–butadiene–styrene improves high-temperature resistance and fatigue properties [13, 14]. Graphene's layered structure may delay oxygen penetration, aiding aging resistance [15].

For enhancing SMA, multi-walled carbon nanotubes (MWCNTs) within a compatible hydrocarbon plasticizer in polymer-modified bitumen could mitigate SMA's temperature sensitivity, bitumen aging, and adhesion loss to mineral aggregates [16]. Several studies explore MWCNTs' effects within polymer–bitumen systems on SMA properties.

According to the authors of [17], adding carbon nanotubes (CNTs) in concentrations of 0.5–1% of the bitumen weight showed minimal impact on Marshall stability, but it did reduce Marshall flow and improved rut depth by 45%. Another study examined the effect of polyphosphoric acid (PPA), CNTs, and styrene–butadiene rubber (SBR) on SMA's moisture resistance, finding that SBR/PPA and CNTs (up to 1.5%) increased strength, elasticity, and durability, but higher CNT levels decreased moisture resistance [18]. A different study [19] observed that adding 2% multi-walled carbon nanotubes (MWCNTs) to asphalt significantly increased deformation resistance and fatigue durability, especially in tropical climates. While all researchers noted improvements in asphalt properties from MWCNTs, higher concentrations (0.5–2%) introduce challenges. This could lead to several negative effects. Higher concentrations of MWCNTs make it difficult to achieve uniform distribution, causing

delamination and degrading the composite's properties. High MWCNT content reduces plasticity due to the nanotubes' strong structuring ability, potentially weakening resistance to temperature-induced deformations. Additionally, high MWCNT concentrations significantly increase the cost of the final composite. Optimization of the carbon nanotube (CNT) content, along with the selection of a compatible hydrocarbon plasticizer that ensures stable dispersion and high interfacial affinity, is a critical task for the practical implementation of this technology. However, current literature lacks systematic studies focusing on the fundamental physicochemical mechanisms governing the interaction between CNTs and the polymer phase of polymer-modified bitumen (PMB) during thermal-oxidative aging.

One of the most degradation-sensitive components of PMB is the thermoplastic elastomer styrene–butadiene–styrene (SBS), whose molecular architecture includes polybutadiene blocks highly susceptible to degradation under oxygen exposure, thermal load, and ultraviolet radiation. According to [20], PMB aging proceeds through a radical chain mechanism, involving the following key stages: hydrogen abstraction from the polymer backbone with the formation of alkyl radicals, scission of double bonds and formation of peroxidic structures, and propagation of chain reactions resulting in molecular weight reduction and breakdown of the macromolecular network. This leads to loss of elasticity, increased brittleness, and deterioration in adhesion properties of the modified binder.

Due to their unique structure, carbon nanotubes (CNTs) exhibit potential for inhibiting polymer degradation. The CNT surface is enriched with a delocalized π-electron system capable of stabilizing alkyl radicals via electron delocalization. Studies [21, 22] have shown that CNTs can act as radical scavengers, reducing the concentration of active species involved in chain degradation of polymers. In [23, 24], it was demonstrated that CNTs can effectively bind free radicals owing to their extended π-conjugated framework, which makes them promising antioxidants for polymer matrices. Specifically, [23] highlighted that multi-walled carbon nanotubes (MWCNTs), particularly those functionalized with hydroxyl groups, outperform single-walled CNTs in radical capture efficiency due to a greater density of structural defects. Furthermore, in [25], a combined experimental and theoretical study using density functional theory (DFT) revealed that the addition of 0.1–0.5 wt.% MWCNTs into a fluorosilicone rubber (FSR) matrix significantly enhances its thermo-oxidative stability through alkyl radical absorption. The antioxidant behavior was attributed to the redistribution of spin density over aryloxy groups and sp^2-hybridized carbon atoms, which interact with highly reactive radical species and effectively neutralize them. These findings underscore the potential of CNTs not only as radical scavengers but also as effective absorbers of reactive oxygen species in polymer-based materials, including construction and road bituminous composites.

Previous research has also indicated that in hydrophobic matrices, such as those found in bitumen and SBS-based systems, CNTs tend to self-assemble into localized nanodomains. This behavior results from a balance of interparticle interactions and significantly influences the rheological properties of the composite [26]. Consequently, the effect of CNTs on the aging resistance of the polymer phase in PMB arises not only from their structural role but also from their electron-accepting capacity and ability to form stable interfacial domains in hydrophobic environments. This evidence shows the need to shift from empirical approaches toward a fundamentally grounded investigation into the impact of CNTs on the kinetics of polymer degradation in PMB. Such research should incorporate thermodynamic analysis of nanocomplex stability and activation energy calculations derived from experimental data. Implementation of this approach will not only enable quantitative evaluation of CNTs' protective effect but also lay the scientific foundation for designing new durable asphalt composites with enhanced service life.

2. METHODS AND MATERIALS

Raw Materials

The following multi-walled carbon nanotube was considered:

Multi-walled carbon nanotubes (MWCNTs) of the "Taunit" series are quasi-one-dimensional nanoscale, thread-like structures made of polycrystalline graphite, mainly cylindrical with an internal channel. Their external diameter ranges from 10 to 30 nm, with a length of over 20 microns and a bulk density from 0.025 to 0.06 g/cm^3.

The following hydrocarbon plasticizers were considered:

Multi-walled carbon nanotubes (MWCNTs) of the "Taunit" series are quasi-one-dimensional nanoscale, thread-like structures made of polycrystalline graphite, mainly cylindrical with an internal channel. Their external diameter ranges from 10 to 30 nm, with a length of over 20 microns and a bulk density from 0.025 to 0.06 g/cm^3.

The following hydrocarbon plasticizers were considered:

(1) Industrial oil I-40A by OilCool, Moscow, Russia—a low-viscosity liquid, a hydrocarbon mix without asphaltenes, commonly used in road construction as a control sample.

(2) Selective oil refining extract by Lukoil-Permneftepererabotka, Perm, Russia, derived from selective oil refining units via phenol purification.

(3) III Vacuum distillate by Lukoil-Nizhegorodnefteorgsintez, Nizhny Novgorod, Russia—a primary distillation product containing a hydrocarbon mixture mostly with carbon atoms ranging from 20 to 30.

The following polymer was considered:

Styrene–butadiene–styrene (SBS), a linear divinyl–styrene thermoplastic elastomer, SBS 30L-01, produced by Voronezhsintezkauchuk, Voronezh, Russia, in accordance with the standard of the organization TU 38.40327-98.

The following bitumen was considered:

Petroleum bitumen grade BND 100/130 from Lukoil's Nizhny Novgorod Refinery, Nizhny Novgorod, Russia, tested in accordance with Russian State Standard R GOST 33133-14 requirements. Laboratory test results on the bitumen's physical and mechanical properties are shown in Table 1.

Table 1. Physical and mechanical characteristics of bitumen grade BND 100–130.

Indicator Name	Russian State Standard GOST R 33133-14	Actual Indicators
Needle penetration depth, 0.1 mm, at a temperature of 25 °C	101–130	112
Needle penetration depth, 0.1 mm, at a temperature of 0 °C	more 30	34
Softening temperature of the ring and ball, °C	more 45	47
Ductility, cm, at 0 °C	more 4.0	5.6
Fragility, °C	less 20	−20
Change in the mass of the sample after aging, %	less 0.7	0.5
Change in the softening temperature of the sample after aging, %	less 7	4

Technology of preparation of polymer-modified binder

(1) In the first stage, a nano-modified dispersion system of "hydrocarbon plasticizer–carbon nanotubes" was prepared. Using an immersion ultrasonic disperser, the mixture was processed until it reached a homogeneous state (details of preparation methods are in the first-phase research report). Separately, bitumen was heated in a sealed container to a working temperature of 160–170 °C. A mixer and heat control sensor were then inserted, and the "hydrocarbon plasticizer–carbon nanotubes" system was gradually added over 2–3 min, with continuous mixing at 200 rpm for another 5–10 min.

(2) In the second stage, the polymer was slowly added to the bitumen containing the nano-modified dispersion system over 3–10 min at a mixing speed of 100 rpm at a temperature mixing of 165–170 °C.

(3) In the third stage, the mixer speed increased to 300 rpm. The container was sealed with a temperature sensor for continuous heat monitoring. Mixing continued until the polymer was uniformly integrated into the bitumen. The modified polymer–bitumen binder was then placed in an oven at 135 °C for 1–2 h to stabilize the binder structure through a "curing" process.

Optimization of the composition of polymer-modified binder

After preparation, all samples of the PMB and PNMBs underwent dynamic viscosity testing using a rotational viscometer (Brookfield viscometer). If the dynamic viscosity was less than 3 Pa·s at a test temperature of 135 °C, the sample was selected for further study. Conversely, samples with viscosities exceeding 3 Pa·s were excluded from subsequent testing.

During the optimization of polymer–bitumen binder control compositions with various hydrocarbon plasticizers, the following designations were established: minimum polymer content as C_P and minimum hydrocarbon plasticizer content as C_{HP}. This approach leverages extensive existing research on polymer-modified compositions with varied components. For hydrocarbon plasticizers, the content range was set at 1.8–2.3%, while for the SBS 30L-01 polymer (a divinyl–styrene thermoplastic elastomer), it was set at 2.8–3.5%. Using approximation, equations were derived to characterize the impact of plasticizer and SBS 30-01L content on binder properties, with coefficients used to calculate optimal content ranges.

Optimization focused on metrics (in accordance with the requirements of Russian State Standard GOST R 52056-2003)

(1) Penetration depth at 25° C (P25) and 0 °C (P0) reflects binder hardness based on resistance to needle penetration at various temperatures, mm−1;

(2) Softening point (Ts) indicates resistance to high temperatures, evaluated by binder deformation under a loaded ball at increasing temperatures, °C;

(3) Fragility temperature (Tfr) reflects the binder's crack resistance at low temperatures, assessed through bending stress on a thin layer, °C;

(4) Ductility at 25 °C (D25) and 0 °C (D0) represents binder plasticity through its ability to stretch at various temperatures, mm;

(5) Elasticity at 25 °C (E25) and 0 °C (E0) indicates the binder's ability to regain shape after load removal, measured as the reduction in the stretched bitumen "tails" relative to the original form (%) after a ductility test, %.

Kinetic effects of multi-walled carbon nanotubes on polymer degradation in modified binder

To quantitatively assess the influence of multi-walled carbon nanotubes (MWCNTs) on the thermo-oxidative stability of the polymer phase in polymer-modified bitumen (PMB), a kinetic modeling approach based on the classical Arrhenius equation was employed. In this context, dynamic viscosity was adopted as a sensitive rheological indicator of the supramolecular structure of the polymer-modified system. Changes in viscosity reflect alterations in the integrity of the spatial network formed by the styrene-butadiene-styrene (SBS) modifier within the bitumen matrix, particularly due to thermal and oxidative chain scission of the polybutadiene blocks.

Dynamic viscosity measurements were carried out using a rotational rheometer (Anton Paar, Austria) with a coaxial cylinder configuration, ensuring stable laminar shear and reproducible viscosity readings. The tests were conducted at 135 °C, a temperature commonly used in binder performance characterization, which provides a balance between sensitivity to structural changes and the minimization of measurement-induced thermal degradation. The oxidative aging process was simulated using the Rolling Thin Film Oven Test (RTFOT) in accordance with Russian State Standard GOST R 33140-2014, over 85 minutes. To evaluate the temperature dependence of degradation kinetics, aging was conducted at three isothermal conditions: 153 °C, 163 °C (standard), and 173 °C. These temperatures were selected to cover a range relevant to real-world production and service conditions of asphalt pavements, without inducing complete loss of the polymer structure.

The degradation of the SBS polymer was modeled as a first-order reaction process, consistent with prior studies [29–31] that have shown chain scission, oxidation, and structural decomposition of PMB to follow first-order kinetics under thermal aging. According to the classical Arrhenius expression, the rate constant k describing the degradation process at a given temperature is given by:

$$k = A \cdot e^{-E_a/RT}, \quad (1)$$

there: k – apparent rate constant of structural degradation, (s^{-1});

A – pre-exponential (frequency) factor, (s^{-1});

E_a – apparent activation energy, (J/mol);

R – the universal gas constant, (8.314 J/(mol·K));

T – absolute temperature, (K).

This equation, initially proposed by Svante Arrhenius in 1889 as an empirical relationship, was later theoretically justified through transition state theory and statistical thermodynamics [27, 28]. Several studies on PMB aging [29-31] have demonstrated that viscosity changes can be approximated as the result of kinetic degradation processes within the polymer supramolecular structure. For instance, [29, 30] show that aging of SBS-modified binders leads to the breakdown of polybutadiene chains, resulting in reduced elasticity, increased brittleness, and a rise in viscosity. These changes can be interpreted using kinetic models such as the Arrhenius equation, where viscosity serves as a function of the degradation rate of the polymer phase. Furthermore, [31] directly links the evolution of rheological parameters with chemical aging processes, including oxidation, chain scission, and the formation of oxygen-containing groups that disrupt the 3D polymer network. In the context of PMB, the Arrhenius model enables indirect quantification of the resistance of the polymer network to oxidative and thermal degradation

Thus, variations in dynamic viscosity (η) over time and under thermal exposure can be quantitatively interpreted as a result of thermally induced degradation processes in the polymer phase of PMB. This enables the use of viscosity as an indirect structural indicator for assessing degradation kinetics and for estimating the effective activation energy of the process. The effective degradation rate constant k was calculated using the following relationship:

$$k = \frac{1}{t} \cdot \ln\left(\frac{\eta_2}{\eta_1}\right), \quad (2)$$

there: η_1 – dynamic viscosity before RTFOT aging;

η_2 – dynamic viscosity after RTFOT aging;

t – aging duration (85 minutes, converted to seconds for consistency with k units);

k – is interpreted as the effective structural degradation rate at a given temperature.

This formulation assumes that the change in viscosity is primarily driven by degradation of the polymer network (e.g., SBS phase), rather than bitumen oxidation alone. While this is a simplification, prior rheological and chemical studies [29-31] suggest that SBS degradation dominates the mechanical property evolution in PMBs during early stages of aging. It is important to note that the Arrhenius-based first-order kinetic model is most accurate during the early stages of oxidative aging, such as those simulated by the RTFOT protocol. Under these conditions, the degradation process is dominated by initial chain scission events in the polybutadiene segments of the SBS polymer, while the contribution of the bitumen matrix remains relatively limited. This justifies the use of dynamic viscosity as a sensitive structural proxy for polymer network integrity. However, at prolonged aging durations or under more severe thermal-oxidative environments, the degradation mechanism may evolve toward more complex or nonlinear kinetics due to progressive oxidation, crosslinking, or secondary network rearrangements. Therefore, the derived kinetic parameters (k, E_a, A) should be interpreted within the temporal scope of short-term aging processes, recognizing that deviations from first-order behavior may occur outside this regime.

The apparent activation energy E_a for each binder composition was obtained by plotting $\ln k$ as a function of $1/T$, where the slope of the linear regression yields $-E_a/R$. Subsequently, the activation energy E_a was calculated from the slope of the linear plot of $\ln(k)$ versus $1/T$, according to:

$$\ln k = \ln A - \frac{E_a}{R} \cdot \frac{1}{T}, \quad (3)$$

This procedure allows for the extraction of the temperature sensitivity of the degradation process, while the intercept provides an estimate of the pre-exponential factor A, reflecting the frequency of successful degradation events.

This kinetic methodology, while phenomenological in nature, offers a practical and reproducible means of comparing the thermo-oxidative stability of different PMB compositions, particularly when

direct chemical analysis of degradation is not feasible. Furthermore, the inclusion of nanomodifiers such as MWCNTs may alter the kinetics by providing steric hindrance, enhancing polymer dispersion, or modifying oxygen diffusion pathways—effects that are indirectly captured in the calculated values of k, E_a, and A.

Mineral materials used for the preparation of stone mastic asphalt concrete:

1. Coarse aggregate: Granite crushed stone (5–20 mm, 3–10 mm) produced by LLC "Mercury", Moscow, was used. All sizes were tested to meet regulatory standards, fulfilling Russian Sate Standard GOST 8267-93 and Russian Sate Standard GOST 7392-02 requirements for physical and mechanical properties.

2. Fine aggregate: Granite sand from crushed stone screenings (0–5 mm) produced by LLC "Mercury" was utilized. This sand, a natural sand–gravel mix, was fully compliant with Russian Sate Standard GOST 31424-2010 in all physical and mechanical properties.

3. Filler: Fine mineral powder MP-1 produced by LLC "Shchelkovo Mining", Moscow, consisting of dolomite sedimentary rock, was used as a filler. This powder passed all required tests, meeting Russian Sate Standard GOST R 52129-2003 for physical and mechanical properties.

4. Stabilizing additive: Stone mastic asphalt differs from conventional asphalt by its high coarse aggregate and bitumen binder content. To retain bitumen on the aggregate's surface, a stabilizing additive was added. Viatop-66 produced by LLC "Rettenmayerrus", a granulated cellulose fiber, was used as the stabilizing additive.

Optimization of the composition of stone mastic asphalt concrete

Designing the composition of asphalt concrete mix involves selecting ratios of mineral components with a specific gradation and organic binder to meet standards for volumetric design requirements (in accordance with GOST R 58406.1-2020). The mineral composition (coarse and fine aggregates) is determined using sieves with nominal mesh sizes of 0.063, 2.0, 4.0, 5.6, 8.0, 11.2, 16.0, 22.4-, and 31.5-mm. Initial gradation is achieved by mixing prepared mineral materials to ensure that the particle size distribution meets standard requirements. Coarse granite aggregate, fine aggregate (crushed rock fines), and mineral powder are sieved and combined to create the mineral framework for SMA-16 stone mastic asphalt, as shown in Table 2.

Table 2. Granulometric composition of the mineral part of stone mastic asphalt concrete SMA-16.

No	Name of Materials	Content, %	Size of Sieves, mm Grain Content Is Smaller Than This Size, % by Weight								
			31.5 mm	22.4 mm	16.0 mm	11.2 mm	8.0 mm	5.6 mm	4.0 mm	2.0 mm	0.063 mm
1	Granite crushed stone of fractions 5–20 mm, 3–10 mm	67.0	67.0	67.0	59.3	32.4	8.0	2.0	1.0	0.0	0.0
2	Granite sand from the screening of the crushing fraction of 0–5 mm	21.0	21.0	21.0	20.23	19.0	18.0	16.0	15.5	13.0	0.9
3	Mineral powder MP-1	12.0	12.0	12.0	12.0	12.0	12.0	11.0	10.8	9.0	7.2
Grain composition of the mineral part, %			100.0	100.0	91.53	63.4	38.0	–	27.3	22.0	8.1
Requirements of Russian State Standard GOST R 58406.1-2020, %			–	100	90–100	50–65	35–50	–	23–38	18–28	7–12

As shown by the data, the aggregate composition meets the requirements of Russian State Standard GOST R 58406.1-2020. To retain bitumen binder on the stone material surface, 0.3% Viatop-66 stabilizing additive was added relative to the mineral component (beyond the mineral fraction's 100%).

Methods of investigation of stone mastic asphalt concrete with polymer-nanomodified binder

The properties of asphalt concrete are assessed using standardized methods outlined in documents governing quality standards, such as the requirements of Russian State Standard GOST R 58406.1-2020 and the requirements of Russian State Standard GOST 9128-2013.

(1) Physical Properties:

- Bulk density (G_{mb}) determines the mass, including pores, per unit volume. It is found by measuring the asphalt sample's weight in air and water. Three samples, cleaned of particles, are weighed in air (m), immersed in 18–22 °C water for four minutes, weighed in water (m_1), and then in air again (m_2).
- Air void content (P_a) represents the air voids in compacted asphalt concrete, calculated based on the bulk and maximum densities.
- Water saturation (W) measures water absorbed under specific conditions, using samples from the bulk density test. These are placed in a vacuum at 2000 Pa for an hour, followed by atmospheric pressure for 30 min. After removing excess water, the air mass (m_3) is measured. Water saturation W is calculated as the difference between m3 and m, related to the material's mass difference between m_2 and m m_1.

(2) Performance Properties:

- Water resistance coefficient for the tensile strength ratio (TSR): This coefficient measures the ratio of indirect tensile strength for specimens exposed to water saturation and freeze–thaw cycling (24 h) to the strength of samples maintained in room conditions.
- Long-term water resistance coefficient (TSR): Determined similarly to the TSR but uses a prolonged freeze–thaw cycle of 60 days.
- Rut depth (resistance to rutting by rolling a loaded wheel) indicates rutting resistance by measuring the rut depth on an asphalt slab subjected to repeated rolling under a set vertical load at 60°C in water.

(3) Additional Indicators:

- Compressive strength at 20 °C and 50 °C reflects the ability to withstand internal stresses from compressive loads at different temperatures, identifying the maximum load at sample failure.
- Tensile strength at splitting assesses asphalt resistance to cracking in low tem-peratures. Samples conditioned in water at 0 °C are subjected to a test where a lateral load is applied to cause splitting.
- Shear stability predicts the asphalt's resistance to dynamic loads from vehicles in real conditions, determined by friction and adhesion coefficients during uniaxial compression and Marshall compression testing (in accordance with requirements of Russian State Standard GOST 31015-2002).– calcium oxide CaO – 58-60%;

Multi-criteria optimization of stone mastic asphalt concrete

The evaluation of asphalt concrete performance necessitates a structured approach grounded in standardized testing methodologies and quantifiable indicators. The physical, mechanical, and durability-related properties described above form the empirical basis for assessing the material's operational suitability under varying service conditions. To systematically interpret these multifaceted properties, a set of partial quality criteria (PQC) was developed. To evaluate the quality of asphalt concrete, a set of partial quality criteria is proposed, corresponding to its functional characteristics. These criteria are normalized to allow integration into a generalized assessment:

1. Physical Properties Criteria:

1.1 QC_1 – Air Void Content

$$PQC_1 = \begin{cases} 1 \\ e^{-k_1(P_a - P_{opt})^2}, \end{cases} \quad \text{if } 2.0 \le P_a \le 4.0 \tag{4}$$

there: Pa – measured air void content in compacted asphalt concrete, (%);

P_{opt} – optimal target value, typically 3%;

k_1 – aging duration (85 minutes, converted to seconds for consistency with k units);

k – penalty coefficient that governs the steepness of the exponential decline (suggested in the range 1.0–1.5 depending on sensitivity).

Air void content is a critical volumetric parameter that affects the durability, permeability, and mechanical integrity of asphalt concrete. According to Russian State Standard GOST R 33140-2014, the allowable range for air voids lies between 2.0% and 4.0%. Values below 2.0% may indicate over-compaction, reducing permeability and increasing the risk of bleeding or deformation. Values above 4.0% suggest insufficient compaction, leading to increased moisture susceptibility and reduced structural stability. Therefore: if Pa in [2.0, 4.0], the material is considered well-compacted, and the criterion is assigned a value of 1. f Pa not in [2.0, 4.0], the exponential penalty function is applied. This approach penalizes deviations from the optimal design air void level, encouraging a balance between durability and resistance to deformation.

1.2 PQC_2 – Water Saturation

$$PQC_2 = 1 - \frac{W}{W_{max}}, \quad (5)$$

there: W – measured water saturation under vacuum and atmospheric pressure;

W_{max} – maximum allowable saturation (usually 2%).

This criterion evaluates the susceptibility of asphalt concrete to water ingress. A lower saturation results in a higher value of the criterion, indicating improved moisture resistance.

1.3 PQC_3 – Bulk Density

$$PQC_3 = \frac{G_{mb}}{G_{mb,ref}}, \quad (6)$$

there: G_{mb} – measured bulk density;

$G_{mb,ref}$ – reference (design) bulk density.

This indicator reflects how closely compacted density aligns with the design density, thus serving as a measure of volumetric stability and quality control.

2. Performance Properties Criteria:

2.1 PQC_4 – Tensile strength ratio (24h)

$$PQC_4 = \frac{TSR_{24h}}{TSR_{min}}, \quad (7)$$

there: $TSR_{24\,h}$ – measured tensile strength ratio of specimens after 24 hours of water saturation and a freeze–thaw cycle;

$TSR_{\min}$ – minimum required value of the tensile strength ratio, which is typically set at 0.80 based on regulatory standards.

This criterion represents short-term water resistance of asphalt concrete. A value exceeding 1 indicates a strength above the required threshold, while values below 1 highlight potential durability concerns.

2.2 PQC_5 – Tensile strength ratio (60 days)

$$PQC_5 = \frac{TSR_{60\,days}}{TSR_{min}}, \quad (8)$$

there: TSR_{60days} – measured tensile strength ratio after 60 days of freeze–thaw cycles.

This criterion indicates long-term moisture and freeze–thaw resistance. It helps to differentiate materials with superior durability under prolonged environmental loading.

2.3 PQC_6 – Rutting Resistance

$$PQC_6 = 1 - \frac{D_{rut}}{D_{max}}, \quad (9)$$

there: D_{rut} – measured rut depth after repeated wheel tracking;

D_{max} – maximum allowable rut depth (usually less than 4 mm).

This metric quantifies resistance to permanent deformation. A higher PQC_6 value implies a lower rut depth and, thus, greater structural stability under traffic loading.

3. Mechanical Strength Criteria:

3.1 PQC_7 – Compressive Strength at 20°C

$$PQC_7 = 1 - \frac{R_{20}}{R_{20,ref}}, \quad (10)$$

there: R_{20} – measured compressive strength at 20°C;

$R_{20,ref}$ – reference strength at 20°C.

This criterion measures load-bearing capacity at moderate temperatures, serving as a baseline for mechanical performance evaluation.

3.2 PQC_8 – Compressive Strength at 50°C

$$PQC_8 = 1 - \frac{R_{50}}{R_{50,ref}}, \quad (11)$$

there: R_{50} – measured compressive strength at 50°C;

$R_{50,ref}$ – reference strength at 50°C.

This parameter assesses thermal stability. It indicates how well the material maintains strength when softened by elevated temperature.

3.3 PQC_9 – Splitting Tensile Strength at 0°C

$$PQC_9 = \begin{cases} 1, \\ e^{-k_9(R_{split} - R_{opt})^2}, \end{cases}$$

$$\text{If } 2.5 \le R_{split} \le 6.0 \text{ otherwise} \quad (12)$$

there: R_{split} – measured is the experimentally measured splitting tensile strength at 0 °C, (MPa);

R_{opt} – optimal target value within the regulatory range,(e.g., 4.25 MPa);

k_9 – penalty coefficient controlling the steepness of the exponential decline, (typically selected in the range 0.2–0.3 based on sensitivity analysis).

This criterion reflects the material's resistance to low-temperature cracking. According to Russian State Standard R GOST 33133-14, the acceptable range for this indicator lies between 2.5 and 6.0 MPa. Both under- and overperformance relative to this range may result in negative consequences: Values below 2.5 MPa indicate insufficient cohesion, leading to brittle fracture under thermal contraction. Values above 6.0 MPa may correspond to excessive stiffness, which reduces the asphalt's flexibility and promotes crack formation. Therefore when Rsplit in [2.5, 6.0], the criterion equals 1, indicating fully satisfactory crack resistance. When Rsplit not in [2.5, 6.0], the exponential penalty function is activated. This reflects the degree of deviation from the optimum and penalizes both excessive stiffness and insufficient strength, thereby preserving a balanced mechanical performance.

3.4 PQC_{10} – Shear Stability:

$PQC_{10.1}$ – Internal Friction Coefficient

$$PQC_{10.1} = \frac{\mu_{meas}}{\mu_{meas,min}}, \quad (13)$$

there: μ_{meas} – measured coefficient of internal friction (dimensionless);

$\mu_{meas,min}$– minimum permissible value (0.93).

This criterion evaluates the internal resistance of the asphalt mixture to shearing deformation due to particle interlock and cohesion. A value greater than or equal to 1 indicates that the frictional component of shear stability meets the regulatory requirements.

$PQC_{10.2}$ – Adhesion Strength at 50 °C

$$PQC_{10.2} = \frac{R_{adh}}{R_{adh,min}}, \quad (14)$$

there: R_{adh} – measured adhesion strength at shear (MPa) at 50 °C;

$R_{adh,min}$ – minimum acceptable adhesion strength (0.18).

This criterion characterizes the asphalt binder's ability to adhere to the mineral skeleton under elevated temperatures. Adhesion loss at high temperatures can lead to slippage and rutting. A value ≥1 indicates adequate adhesive performance.

To enable integration into the Generalized Effectiveness Coefficient (GEC), an arithmetic mean of these two sub-criteria was used to represent the overall PQC_{10} value. This averaging approach is justified by the comparable functional role of both parameters in characterizing shear resistance and stability under high-temperature loading conditions. Therefore, in the final multi-criteria optimization framework, $PQC_{10}=(PQC_{10.1}+PQC_{10.2})/2$.

Generalized Effectiveness Coefficient (GEC):

To consolidate the performance across all criteria, a generalized effectiveness coefficient (GEC) is introduced as the root mean square of normalized partial criteria:

$$GEC = \sqrt{\frac{1}{n}\sum_{i=1}^{n}(PQC_i)^2} \quad (15)$$

This formulation: gives proportionally greater weight to higher-performing criteria; allows moderate deviations without critical penalization; ensures that each component contributes meaningfully to the overall quality index.

3. RESULTS AND DISCUSSION

3.1. Optimization of the Composition of Polymer-Modified Binder

Bitumen is a temperature-sensitive material, and viscosity is one of its most critical parameters, serving as a measure of its resistance to flow and significantly influencing workability. The viscosity of the PMB and PNMB was evaluated at 135 °C. The results showed that the viscosity of all samples of the binders complied with Superpave specifications (ASTM D6373) (i.e., ≤3000 cP) and was sufficiently fluid to enable pumping during the operation of asphalt mixing plants. A series of experiments yielded the following relationships for the properties of polymer–bitumen binder prepared with industrial oil I-40A as the hydrocarbon plasticizer. These relationships are presented in Table 3. The data in this table detail how specific binder properties, such as hardness, elasticity, and temperature resistance, respond to variations in the binder's composition and processing conditions. The results help optimize the performance of the asphalt binder in meeting durability and stability requirements for road construction.

Table 3. Dependences of the properties of the control composition of PMB 60, prepared on the basis of industrial oil grade I-40A.

Name of the Indicator	Requirements of Russian State Standard GOST R 52056-2003	No. of composition of polymer-modified binder (PMB 60)											
		1	2	3	4	5	6	7	8	9	10	11	12
Hydrocarbon Plasticizer Content C_{HP}, %	–	2.3				2.0				1.8			
Polymer Content C_P, %	–	2.8	3.0	3.2	3.5	2.8	3.0	3.2	3.5	2.8	3.0	3.2	3.5
Penetration Depth at 25 °C P_{25}, mm^{-1}	more 60	79	72	71	66	88	86	79	64	60	54	52	46
Penetration Depth at 0 °C P_0, mm^{-1}	more 32	52	47	42	31	56	53	46	31	22	19	16	16
Softening Point Ts, °C	more 54	53	58	57	64	54	57	55	64	52	61	69	60
Fragility Temperature T_{fr}, °C	less –20	–20	–20	–23	–24	–24	–23	–23	–23	–22	–22	–19	–20
Ductility at 25 °C D_{25}, m	more 25	51	56	58	64	45	44	48	54	50	42	35	35
Ductility at 0 °C D_0, mm	more 11	17	19	22	23	16	16	19	18	13	12	10	10
Elasticity at 25 °C E_{25}, %	more 80	68	72	74	80	50	53	73	71	68	70	74	76
Elasticity at 0 °C E_0, %	more 70	62	61	71	73	42	40	65	65	64	66	68	72

Using approximation, equations were derived to describe the influence of industrial oil I-40 A and SBS 30-01L polymer content on the properties of the polymer-modified binder. Coefficients in these equations: $\boldsymbol{f(x) = ax^2 + bx + c}$, where x is the content of SBS 30-01L, %. The selection of a quadratic equation was based on the observed experimental data, which demonstrated a nonlinear dependency between the polymer and plasticizer content and the corresponding properties of the binder. Upon plotting the results, we noticed that a quadratic relationship provided the best fit, as it adequately captured the trends and interactions between the variables. This was further confirmed by the high coefficients of determination (R^2 values) obtained during the approximation process. We believe that the quadratic model allows for a more accurate and reliable description of the complex dependencies in the system under study. The coefficients in these equations capture the specific impact of the SBS polymer and plasticizer content and are presented in Table 4.

Table 4. Coefficients of the equation of dependence of changes in the properties of PMB 60, prepared on the basis of industrial oil grade I-40A.

Name of the Indicator	Coefficients of the Dependence Equations								
	1.8			2.0			2.3		
	a	b	c	a	b	c	a	b	c
P_{25}, mm^{-1}	−36.14	198.31	–175.0	–11.97	54.35	–3.38	–6.98	28.44	51.95
P_0, mm^{-1}	−33.95	188.3	−193.3	16.80	−104.09	191.28	−15.90	81.15	−41.30
Ts, °C	11.81	−64.7	137.0	−65.30	451.08	−661.92	−0.65	16.34	11.43
T_{fr} °C	−6.43	53.5	−113.1	−6.43	52.48	−111.07	−12.79	15.54	−41.74
D_{25}, mm	11.97	−54.3	107.4	54.54	−355.87	628.31	−3.84	50.74	−54.90
D_0, mm	−17.75	132.6	−181.9	−4.34	16.07	−7.75	−13.07	87.41	−135.41
E_{25}, %	−42.23	306.1	−472.2	−25.53	167.43	−204.93	1.59	0,17	46.17
E_0, %	−28.82	226.0	−361.5	−1.39	13.67	35.85	−5.09	45.41	−31.32

The coefficients were obtained through a regression analysis of the experimental data. Using the measured properties of the polymer-nanomodified binder (PNMB 60) at different compositions of hydrocarbon plasticizer (C_{HP}) and SBS polymer, we approximated the dependencies of each property on the content of these components. A quadratic equation was selected as the most appropriate model, as it provided the best fit to the experimental data. The regression process yielded the coefficients a, b, and c, which describe the influence of the SBS polymer and hydrocarbon plasticizer content on each property. These coefficients were calculated separately for each level of C_{HP} content (1.8%, 2.0%, and 2.3%) to reflect the specific effects at different compositions. Using the coefficients provided in Table 3, the optimal ranges of industrial oil I-40 A and SBS 30-01L polymer content were calculated. This optimal range for the components will ensure that the polymer–bitumen binder PMB 60 meets all physical and mechanical property standards in accordance with requirements of Russian State Standard GOST R 52056-2003.

$$C_f = \frac{-b \pm \left(b^2 - 4ac(c-Y)\right)^2}{2a}, \quad (16)$$

there: Y – represents the minimum/maximum allowable value of the PMB 60 property according to Russian State Standard GOST R 52056-2003;

a, b, and *c* – coefficients in the equation characterizing the effect of the properties of PMB 60 (Table 3).

Thus, the optimal range of hydrocarbon plasticizer and polymer content for PMB 60 corresponds to

$$C_{опт} \in [Cf, 2, min_{f,1,max}], \quad (17)$$

there: $C_{f,1}$ and $C_{f,2}$ – denote the left and right boundaries of the polymer concentration range.

Analyzing the results (Table 5), it can be concluded that the optimal SBS 30L-01 polymer content is between 4.2% and 4.5%, while the optimal concentration of industrial oil I-40A is 2.3%.

Table 5. The range of optimal component content in the composition of PMB 60, prepared on the basis of industrial oil grade I-40A.

Name of the Indicator	Ranges of Acceptable Polymer Concentrations, % for PMB 60 with Different Plasticizer Content, %					
	1.8		2.0		2.3	
	Bottom	Up	Bottom	Up	Bottom	Up
P_{25}, mm^{-1}	1.76	3.58	2.21	2.64	0.33	3.86
P_0, mm^{-1}	1.83	3.51	4.27	2.36	1.20	3.52
Ts, °C	2.72	2.41	2.80	3.65	2.71	20.47
T_{fr} °C	–	–	–	–	2.81	4.50
D_{25}, mm	–	–	–	–	1.92	8.82
D_0, mm	2.61	3.93	1.78	3.33	2.55	4.75
E_{25}, %	–	–	–	–	−3.60	3.50
E_0, %	–	–	3.52	6.28	4.20	7.65
$C_{optimal}$	–	–	–	–	4.20	4.50

Using the proposed approach (Tables 3–5, Formulas (1) and (2)) for determining optimal component ranges, an ideal composition was identified for PMB 60 polymer-modified binders based on selective oil refining extract (SORE) (Table 6) and the III vacuum distillate (III VD) (Table 7).

Table 6. The range of optimal component content in the composition of PMB 60, prepared on the basis of extracts of selective oil purification.

Name of the Indicator	Ranges of Acceptable Polymer Concentrations, % for PMB 60 with Different Plasticizer Content, %					
	1.8		2.0		2.3	
	Bottom	Up	Bottom	Up	Bottom	Up
P_{25}, mm^{-1}	1.03	3.75	2.76	3.58	2.01	2.51
P_0, mm^{-1}	1.35	3.78	2.83	4.51	3.27	2.33
Ts, °C	3.21	18.57	–	–	4.61	4.75
T_{fr} °C	3.55	4.30	–	–	–	–
D_{25}, mm	1.97	9.82	2.52	2.21	–	–
D_0, mm	2.05	4.97	2.51	3.63	1.58	3.13
E_{25}, %	−3.30	3.61	2.35	3.01	–	–
E_0, %	4.20	7.21	–	–	3.02	7.08
$C_{optimal}$	4.20	4.30	–	–	–	–

Table 7. The range of optimal component content in the composition of PMB 60, prepared on the basis of III vacuum shoulder strap.

Name of the Indicator	Ranges of Acceptable Polymer Concentrations, % for PMB 60 with Different Plasticizer Content, %					
	1.8		2.0		2.3	
	Bottom	Up	Bottom	Up	Bottom	Up
1	2	3	4	5	6	7
P_{25}, mm^{-1}	1.54	3.59	1.01	3.65	3.06	3.58
P_0, mm^{-1}	1.87	3.91	1.18	3.24	2.09	4.23
Ts, °C	2.87	2.87	2.75	19.23	–	–
T_{fr} °C	–	–	2.78	4.40	–	–
D_{25}, mm	–	–	1.89	8.67	–	–

Continuation of Table 7

D_0, mm	–	–	3.03	4.70	2.52	2.45
E_{25}, %	–	–	−2.23	3.21	2.53	4.01
E_0, %	2.89	4.02	4.20	5.78	2.05	3.23
$C_{optimal}$	–	–	4.20	4.40	–	–

Analyzing the obtained results (Table 6) reveals that the optimal SBS 30L-01 polymer content in the mixture ranges from 4.2% to 4.3%, with the optimal concentration of selective oil refining extract at 1.8%. For PBV mixtures with III vacuum distillate, the optimal SBS 30L-01 polymer content is between 4.2% and 4.4%, and the III vacuum distillate concentration is 2.0% (Table 7).

3.2. Kinetic effects of multi-walled carbon nanotubes on polymer degradation in modified binder

To quantitatively assess the oxidative-thermal stability of the polymer phase in polymer-modified bitumen (PMB), a first-order kinetic model based on the Arrhenius equation was employed. Dynamic viscosity was used as a structural indicator and was measured before ($\boldsymbol{\eta_1}$) and after ($\boldsymbol{\eta_2}$) accelerated aging using the RTFOT method at three temperatures (153, 163, and 173 °C). Changes in viscosity were interpreted as a result of progressive degradation of the polymeric network formed by the SBS modifier within the bitumen matrix. The compositions of the polymer nanomodified binders (PNMB) are listed in Table 8. The measured values of dynamic viscosity before and after aging are presented in Table 9. Based on these data, effective degradation rate constants and activation energies were calculated, reflecting the relative resistance of the various compositions to thermal degradation of the polymer phase. The effective kinetic parameters derived for the polymer nanomodified binders (PNMB), based on dynamic viscosity measurements before and after RTFOT aging, are summarized in Table 10. These parameters include the apparent degradation rate constants at four aging temperatures, the corresponding activation energies (E_a), and the pre-exponential factors (A), characterizing the temperature dependence of degradation processes in each binder composition.

Table 8. Component composition of PNMB 60.

Composition	Name of the Components of the PNMB Content, %					
	Bitumen Grade BND 100/130	SBS 30L01	Industrial Oil I-40A	Extract of Selective Oil Purification	III Vacuum Fraction	MWCNT
No. 1	100	4.2	2.3	–	–	–
No. 2	100	3.2	2.3	–	–	0.005
No. 3	100	4.2	–	1.8	–	–
No. 4	100	3.2	–	1.8	–	0.005
No. 5	100	4.2	–	–	2.0	–
No. 6	100	3.2	–	–	2.0	0.005

Table 9. Dynamic viscosity of PNMB 60 measured before and after RTFOT ageing.

Composition	Aging temperature, °C							
	153		163		173		183	
	η_1	η_2	η_1	η_2	η_1	η_2	η_1	η_2
1	2	3	4	5	6	7	8	9
No. 1	1.02	1.13	1.02	1.25	1.02	1.41	1.02	2.08
No. 2	0.89	0.95	0.89	0.98	0.89	1.12	0.89	1.45
No. 3	1.12	1.15	1.12	1.18	1.12	1.23	1.12	1.4
No. 4	1.09	1.12	1.09	1.13	1.09	1.15	1.09	1.26
No. 5	1.15	1.18	1.15	1.21	1.15	1.25	1.15	1.39
No. 6	1.13	1.15	1.13	1.17	1.13	1.19	1.13	1.25

Table 10. The kinetic parameters reflecting the relative resistance of PNMB 60 to thermal degradation of the polymer phase.

Composition	Name of the Components of the PNMB Content, %					
	k_{153} x10^{-5}, 1/c	k_{163} x10^{-5}, 1/c	k_{173} x10^{-5}, 1/c	k_{183} x10^{-5}, 1/c	Activation energy, E_a, kJ/mol	The pre-exponential multiplier, A x10^5, 1/c
No. 1	2.01	3.99	6.35	13.97	93.14	6.84
No. 2	1.28	1.89	4.51	9.57	84.28	5.14
No. 3	0.52	1.03	1.84	4.38	75.52	1.26
No. 4	0.52	0.71	1.05	2.84	87.07	0.83
No. 5	0.51	1.00	1.64	3.71	65.74	0.36
No. 6	0.34	0.68	1.02	1.98	91.23	0.27

The results reveal notable differences in the oxidative–thermal stability of the polymer phase among the PNMB compositions. Composition No. 1, which includes a conventional SBS-modified binder without additives, exhibits the highest degradation rate constants and the highest activation energy (93.14 kJ/mol), along with a relatively large pre-exponential factor A (6.84×10^5 s^{-1}). This suggests that although a high energy input is required to initiate degradation, the molecular environment in this formulation facilitates frequent and effective molecular collisions, accelerating structural breakdown once thermal thresholds are exceeded. Composition No. 2, modified with multi-walled carbon nanotubes (MWCNTs), displays lower rate constants and a slightly reduced activation energy (84.28 kJ/mol), while retaining a high pre-exponential factor A (5.14×10^5 s^{-1}). The presence of MWCNTs appears to alter degradation kinetics through a dual mechanism: (i) reinforcement of the SBS-binder network, and (ii) restriction of oxygen diffusion due to increased tortuosity of the nanostructured matrix. These effects align with previous studies, which demonstrate that carbon nanotubes can reduce oxidative aging and enhance the viscoelastic stability of modified binders by acting as nano-reinforcements and diffusion barriers [32-35].

Compositions No. 3 and 4, containing Selective oil refining extract (SORE) extract – without and with MWCNTs—exhibit further reductions in degradation rate constants. In particular, Composition No. 4 (SOP + MWCNT) shows a high activation energy (87.07 kJ/mol) and the lowest A-value among SOP-modified systems (0.83×10^5 s^{-1}), indicating a kinetically hindered degradation mechanism. The reduced frequency factor may be attributed to the synergistic effect of MWCNTs and polar compounds in SOP, which restrict chain mobility and suppress free radical propagation [33,34]. Compositions No. 5 and 6, modified with vacuum distillates(VR), demonstrate the lowest degradation rate constants across the entire temperature range. Composition No. 6 (VR + MWCNT) achieves both the lowest k-values and the smallest A (0.27×10^5 s^{-1}), while still maintaining a high activation energy (91.23 kJ/mol). This combination suggests strong structural stabilization, possibly due to steric hindrance and decreased oxidative accessibility, further enhanced by nanotube-induced matrix reinforcement [32, 35].

Taken together, these results show that the introduction of MWCNTs consistently leads Taken together, these results confirm that MWCNTs consistently reduce the pre-exponential factor A across different formulations, indicating suppressed effective collision frequency and increased resistance to degradation. This supports the hypothesis that MWCNTs enhance structural integrity and reduce oxidative reactivity. Furthermore, their combination with functional modifiers like SOP and VD provides the most favorable kinetic profile—low degradation rates and high activation energies—consistent with advanced strategies for designing durable polymer-modified binders in high-temperature applications [32-35].

3.3. Optimization of the Composition of Stone Mastic Asphalt Concrete

Material properties are closely linked to composition and structure, emphasizing the need to establish a rational bitumen content. Based on sieve analysis (Table 2), an optimal mineral composition for SMA-16 was determined. The mineral portion totals 100%, with additional

bituminous binder calculated beyond this. According to Russian State Standard GOST R 58406.10 requirements, initial bitumen content was calculated based on the bulk density of mineral fillers, including absorbed bitumen. This initial bitumen content was found to be 6.5%. Nine SMA mixtures were prepared using various hydrocarbon plasticizers in the polymer–bitumen binder, as follows:

(1) Bituminous binder content of 6%;
(2) Bituminous binder content of 7%;
(3) Bituminous binder content of 7.5%.

To determine the optimal binder content, the bulk density (G_{mb}), maximum density (G_{mm}), air voids (P_a) (it must be in the range from 2 to 4 %), and voids in the mineral aggregate (*VMAs*) (it must be less than 16%) were measured for the samples. It was found that the plasticizer type did not impact binder optimization, so average results are presented in Fig. 1 and 2.

Analysis of the obtained data (Fig. 1 and 2) allowed for the determination that the optimal polymer-modified binder content in the composition of stone mastic asphalt concrete (SMA-16) lies within the range of 6.9% to 7.15%. Therefore, for further research, the average value of 7% is taken. The percentage of air voids on the binder content is 3.8%.

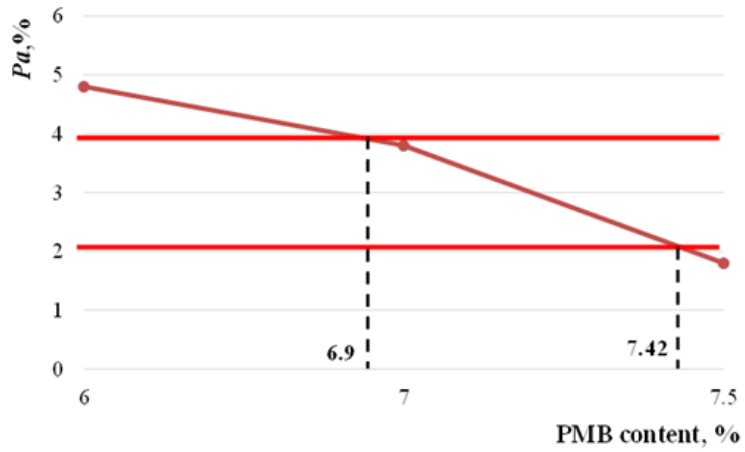

Fig. 1. The effect of the percentage of PMB 60 on the content of air voids, Pa, %.

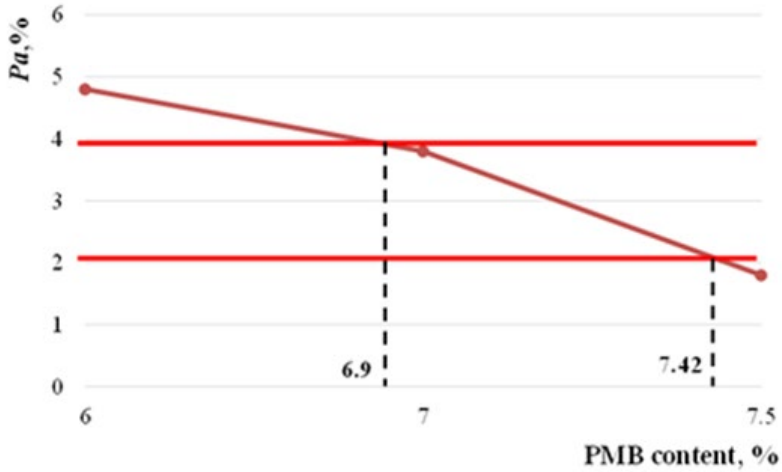

Fig. 2. The effect of the percentage of PMB 60 on the content of voids in the mineral filler, PMZ, %.

3.3. Investigation of Stone Mastic Asphalt Concrete with Polymer-Nanomodified Binder

To determine the effect of the developed polymer-nanomodified binders on the properties of SMA-16, asphalt concrete samples were prepared in quantities of at least three for each experiment, as shown in Fig. 3.

a) Determination of the water resistance coefficient

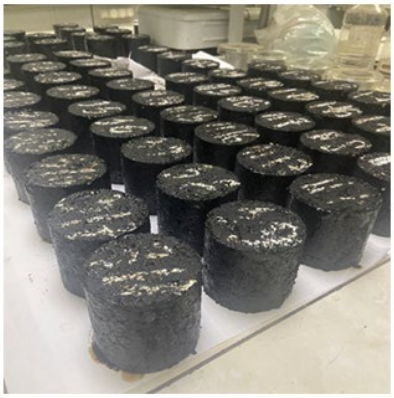

b) Determination of additional physical and mechanical properties

Fig. 3. Samples of stone mastic asphalt concrete to determine (a) the coefficient of water resistance and (b) additional physical and mechanical properties.

The differences between the studied compositions are concluded only in the polymer-modified binders. Previously, the authors selected the optimal content of the polymer-nanomodified binder (PNMB) [16] but with different plasticizers and bitumen. It was also established that it is possible to reduce the polymer content. Therefore, this study will examine the impact of MWCNTs on the properties of asphalt concrete, along with the possibility of reducing the polymer content in the modifying binder. The component composition of the optimized SMA and polymer-nanomodified binder compositions is presented in Tables 11 and 12.

Table 11. The component composition of the stone mastic asphalt concrete mixture SMA-16.

Name of the Components of the Stone Mastic Mixture	Composition Number of SMA-16, the Content of Components, %					
	No. 1	No. 2	No. 3	No. 4	No. 5	No. 6
Coarse Aggregate	67					
Fine Aggregate	21					
Filler	12					
Stabilizing Additive	0.3 of the mineral part (over 100%)					
PNMB	7 of the mineral part (over 100%)					

Table 12. Component composition of PNMB 60 for stone mastic asphalt concrete mixture SMA-16.

Composition Number of SMA-16	Name of the Components of the PNMB Content, %					
	Bitumen Grade BND 100/130	SBS 30L01	Industrial Oil I-40A	Extract of Selective Oil Purification	III Vacuum Fraction	MWCNT
1	2	3	4	5	6	7
No. 1	100	4.2	2.3	–	–	–
No. 2	100	3.2	2.3	–	–	0.005
No. 3	100	4.2	–	1.8	–	–
No. 4	100	3.2	–	1.8	–	0.005
No. 5	100	4.2	–	–	2.0	–
No. 6	100	3.2	–	–	2.0	0.005

The results of determining the physical and performance properties of the studied SMA-16 samples are presented in Table 13, while the additional physico-mechanical property data are shown in Table 14.

Table 13. Physical and performance properties of the studied samples of SMA-16.

Name of the Property Indicator	Requirement of Russian State Standard GOST R 58406.1-2020	Composition Number of SMA-16, Actual Values					
		No. 1	No. 2	No. 3	No. 4	No. 5	No. 6
Physical properties							
Bulk density, *Gmb*, %	–	2.57	2.57	2.56	2.56	2.56	2.56
Content of air voids, *Pa*, %	from 2.0 to 4	3.6	3.6	3.5	3.5	3.5	3.5
Water saturation	–	2.2	1.9	1.8	1.4	1.9	1.4
Performance properties							
Tensile strength ratio, *TSR*	more 0.85	0.88	0.92	0.90	0,96	0,90	0.95
Long-lasting tensile strength ratio, TSR_{60} (60 days)	–	0.52	0.79	0.63	0.86	0.62	0.85
Rut depth, resistance to rutting by rolling a loaded wheel, mm	less 4.0	3.8	2.5	2.6	1.6	2.7	1.8

Table 14. Additional physical and mechanical properties of the studied samples of SMA-16.

Name of the Property Indicator	Requirement of Russian State Standard GOST 9128-2013	Composition Number of SMA-16, Actual Values					
		No. 1	No. 2	No. 3	No. 4	No. 5	No. 6
Additional properties							
Compressive strength, MPa							
at a temperature of 20 °C	more 2.2	2.8	3.2	3.1	4.5	3.1	4.5
at a temperature of 50 °C	more 0.65	1.3	2.4	1.9	2.9	2.0	3.2
Tensile strength at splitting at a temperature of 0 °C, MPa	from 2.5 to 6.0	2.9	3.4	3.2	3.9	3.1	4.2
Shear stability							
– according to the coefficient of internal friction	more 0.93	0.98	0.98	0.98	0.99	0.99	0.99
– by adhesion at shear at 50 °C, MPa	more 0.18	0.45	0.62	0.40	0.95	0.41	1.00

As can be seen from the presented data (Table 13), the introduction of the MWCNTs and the type of hydrocarbon plasticizers (compositions No. 2, No. 4, and No. 6) have no impact on the bulk density and air void content. These characteristics depend on the selected granulometric composition, and their values indicate that all technological operations in the preparation of the SMA-16 samples were properly followed, thus excluding the influence of these factors on the final result.

Stone mastic asphalt concrete is a composite with increased porosity, so the primary failure occurs after prolonged contact with water. When the composite contacts water, the diffusion of water molecules into the bitumen film can occur, leading to the detachment of the bitumen film from the stone surface. This, in turn, causes micro defects that reduce the strength characteristics of the composite, resulting in crack formation and premature failure. Water saturation indicates the ability of the PNMB film formed on the stone material's surface to resist water penetration, which could otherwise destroy the composite from the inside. The introduction of compatible and stable dispersed systems with nanoclusters in the polymer-modified binder improves water resistance by up to 27%.

The TSR (tensile strength ratio) coefficient characterizes the ability of the composite to maintain its strength properties under the prolonged “freeze–thaw” cycle, simulating real-life road conditions during temperature fluctuations around 0 °C in winter and spring–winter periods with increased humidity. This has a particularly negative impact on the durability of the pavement. To strengthen testing conditions, a long-term water resistance coefficient was studied, where the “freeze–thaw” cycle lasted 60 days instead of 24 h. The experiment showed that all the SMA-16 compositions met the required standards for the indicator of the TSR, as shown in Fig. 4.

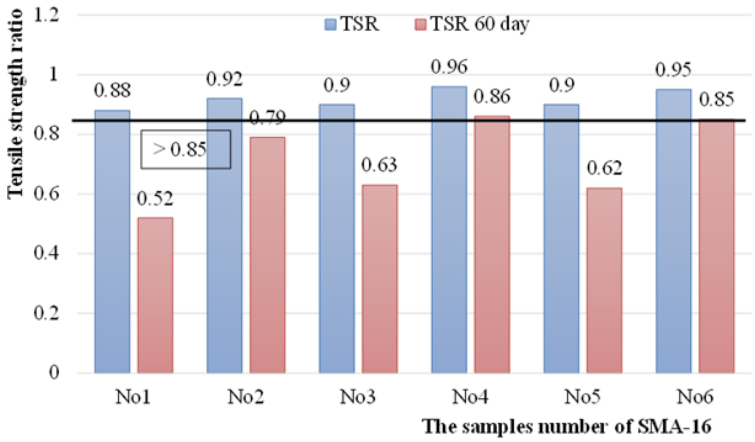

Fig. 4. The effect of the component composition of polymer–bitumen binders on the tensile strength ratio of stone mastic asphalt concrete SMA-16.

However, when samples of stone mastic asphalt concrete are subjected to long-term exposure in aggressive conditions without the introduction of a nanomodified binder, their strength characteristics deteriorate by 30-41%. On the other hand, additional localized multiple structuring of the binder containing a stable dispersed system with nanoclusters helps to further structure and strengthen the binder films on the stone material, reducing the strength to only 10-14%. It is also worth noting that the use of selective oil refining extract (composition No. 4) and III vacuum distillation (composition No. 6) as hydrocarbon plasticizers with MWCNTs helps form a structured system that preserves the strength characteristics of the asphalt concrete within the required range, even after prolonged aggressive loading.

When studying the impact of polymer-modified binders on the strength characteristics of stone mastic asphalt concrete at different temperatures, it was found that all studied compositions meet regulatory requirements. However, using industrial oil combined with MWCNTs (composition No. 2) improves strength by 14% at normal conditions (20 °C), 84% at elevated temperatures (50 °C), and enhances low-temperature crack resistance by 17%. Using selective oil refining extract (composition No. 4) with a MWCNT improves strength by 45% at normal conditions, 80% at elevated temperatures, and 21% for low-temperature resistance. Using III vacuum distillation with a MWCNT (composition No. 5) improves strength by 45% at normal conditions, 60% at elevated temperatures, and 35% for low-temperature resistance. The observed improvements in the strength of stone mastic asphalt concrete prepared with PNMB result from enhanced high- and low-temperature binder properties and increased shear viscosity, indicating greater binder structuring.

The preparation of stone mastic asphalt concrete samples involves compacting the mixture under pressure, which brings the mineral materials closer together within the composite structure. Simultaneously, other processes occur in the composite. The contact between mineral materials happens in the zone of the adsorptive solvent shells of the binder, which are characterized by increased viscosity. This leads to increased internal friction within the road composite. This explains the dependency of the deformation characteristics of the asphalt concrete on the internal friction coefficient. The magnitude of this coefficient directly depends on the surface area and the configuration of the stone material grains in the composite, while the adhesion between the bitumen

binder and the stone material depends on the bitumen quality. Since asphalt concrete is a road composite, its properties are temperature-dependent, and the shear stability coefficient, determined at 50 °C, indirectly characterizes the resistance of stone mastic asphalt concrete to deformation failures caused by dynamic loads from passing vehicles (Fig. 5).

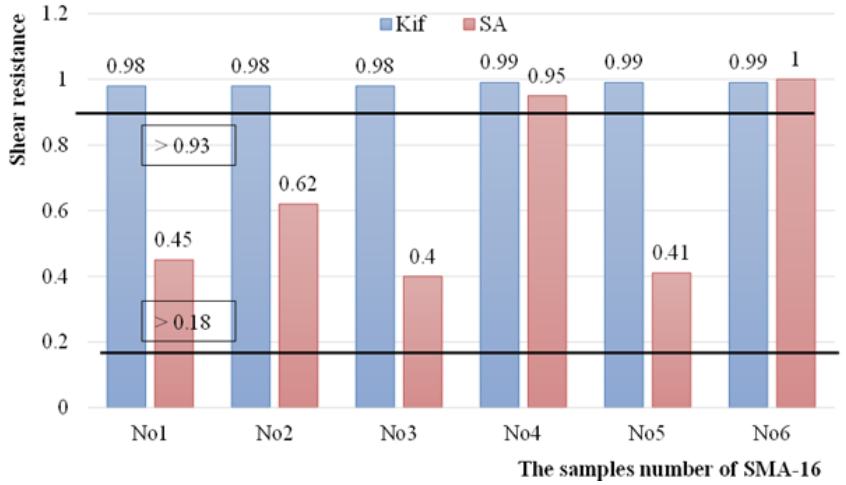

Fig. 5. The influence of the component composition of polymer-nanomodified binders on shear stability; coefficient of internal friction (Kif) and shear adhesion (SA, MPa) of crushed stone mastic asphalt concrete SMA-16.

As seen from the provided data (Fig. 5), the component composition of polymer-nanomodified binders does not significantly affect the internal friction coefficient, which is primarily determined by the characteristics of the mineral material grains and their arrangement in the composite (properly selected gradation). However, the introduction of the MWCNTs significantly improves the shear adhesion, with an increase of up to 240%. This indicates a significant increase in the elastic component of the road composite, enhancing its resistance to shear and the formation of plastic shifts and deformations in road pavements.

The study of the road composite's ability to resist plastic rutting caused by dynamic loads combined with aggressive factors (water and high temperature) is an important part of evaluating the effectiveness of the developed solution. One such method is the measurement of rut depth. The results of experimental studies on the rutting resistance of the stone mastic asphalt concrete samples (SMA-16), in terms of their resistance to plastic deformation from dynamic loads, are presented in Figure 6. The graph numbers in the figure correspond to the sample compositions of SMA-16 (Tables 11 and 12).

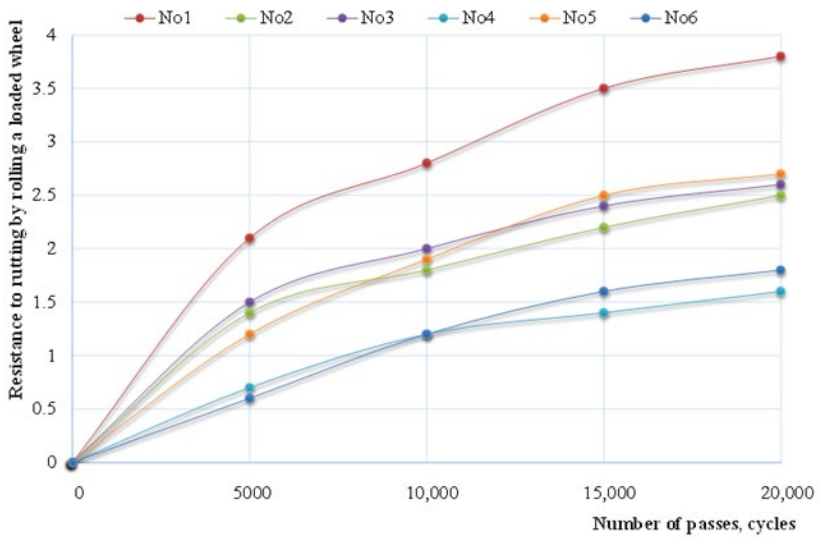

Fig. 6. The influence of the component composition of polymer-nanomodified binders on the rutting resistance of stone mastic asphalt concrete SMA-16.

To analyze the obtained dependencies (Fig. 6) and obtain accurate results, static modeling is used. This method involves performing formal operations to select an approximating function. However, this often leads to models chosen based on variance adequacy values, which may not reflect the actual deformational and rheological characteristics of the studied object. It is well-known that the process of rut formation on road pavements occurs in three stages, namely pre-compaction, plastic rutting, and the destruction of the road composite (asphalt concrete). Therefore, for the experimental dependencies of rut depth formation with respect to the number of wheel load cycles, an exponential model was chosen, which most accurately describes the occurring processes (structural changes) during rut formation in the studied SMA-16 asphalt compositions. This exponential model relies on the following postulates: the rate of rut formation at the initial stage is a finite positive value, which in turn does not depend on the number of loaded wheel passes (cycle); for the fixed wheel passes recorded during the study, there exists an asymptote, which has the following equation:

$$y = k_{\infty}x + b_{\infty} \tag{18}$$

At the last stage of the test, the stone mastic asphalt concrete is compacted and the speed of the rutting formation is stabilized. All these factors form a closed system, which is characterized by the following three-parameter dependence:

$$H = H(N) = a\left(\frac{2}{1+e^{-bN}} - 1\right) + cN, \tag{19}$$

there: $H(N)$ – rut depth after the *Nth* cycle;

a, b, and c – empirical coefficients determined on the basis of experimental data obtained during the test.

Based on the information provided, the values of the model parameters were calculated as $H(N)$; the calculation results are presented in Table 15.

Table 15. Values of model parameters *H(N)*.

Composition Number of SMA-16	Value of Empirical Coefficients		
	a	b	c
1	2	3	4
No. 1	3.817	0.611	0.212
No. 2	2.390	0.434	0.085
No. 3	2.689	0.524	0.113
No. 4	1.622	0.311	0.052
No. 5	2.789	0.564	0.198
No. 6	1.732	0.321	0.057

A joint analysis of the experimental data on the influence of the polymer-nanomodified binder composition in stone mastic asphalt on rut depth formation (Fig. 6) and the calculated parameters of the chosen model *H(N)* reveals the following: parameter *a* represents the maximum rut depth; parameter *b* describes the duration of the pre-compaction stage of the asphalt during road use; and parameter *c* characterizes the rate of rut formation after pre-compaction. Thus, using selective oil refining extract (composition No. 4) and III vacuum distillation (composition No. 6) combined with a MWCNT ensures the formation of a strong, structured system at the binder–mineral interface, significantly reducing rut depth and slowing down rut formation, improving road durability.

In conclusion, by controlling the structure formation of stone mastic asphalt, it is possible to form a reinforced structure through multiple local hardening with a MWCNT and compatibility hydrocarbon plasticizers, leading to durable interlayers on the stone surface that are resistant to dynamic and temperature stresses, thereby improving the longevity of the asphalt pavement.

3.4 Multi-Criteria Optimization of Nanomodified Stone Mastic Asphalt Concrete

The development of high-performance stone mastic asphalt (SMA) mixtures requires a balanced optimization of physical, mechanical, and durability characteristics. Conventional single-parameter assessments are insufficient to capture the complex, interdependent behavior of modern polymer-modified binders—especially those enhanced with nanomaterials. Therefore, a multi-criteria optimization (MCO) approach was employed to evaluate the integrated performance of SMA-16 mixtures modified with various plasticizers and multi-walled carbon nanotubes (MWCNTs). This approach is based on a system of partial quality criteria (PQC), each corresponding to a key functional property of the asphalt concrete (e.g., moisture resistance, mechanical strength, thermal stability, and rutting resistance). To derive an overall performance metric, a generalized effectiveness coefficient (GEC) was introduced using a root mean square formulation, which ensures sensitivity to deviations and rewards balanced performance across all criteria.

Results of Partial and Generalized Criteria Calculations

Table 16 summarizes the calculated values of PQC_1–PQC_{10} for all tested SMA-16 compositions based on experimental data. The corresponding GEC values are presented to reflect the integrated performance.

Table 16. Calculated partial quality criteria (PQC) and generalized effectiveness coefficient (GEC) for SMA-16 compositions.

Composi-tions	Value of PQC and GEC										
	PQC_1	PQC_2	PQC_3	PQC_4	PQC_5	PQC_6	PQC_7	PQC_8	PQC_9	PQC_{10}	GEC
No. 1	1.00	0.82	1.00	1.04	0.65	0.71	1.27	2.00	1.00	1.05	1.19
No. 2	1.00	1.05	1.00	1.09	0.99	1.08	1.45	3.69	1.00	1.63	1.64
No. 3	1.00	1.11	1.00	1.06	0.79	1.06	1.41	2.92	1.00	1.08	1.49
No. 4	1.00	1.43	1.00	1.13	1.08	1.50	2.04	4.46	1.00	1.78	2.31
No. 5	1.00	1.05	1.00	1.06	0.78	1.04	1.41	3.08	1.00	1.09	1.15
No. 6	1.00	1.43	1.00	1.12	1.06	1.48	2.04	4.92	1.00	1.81	2.45

The comparative analysis of the results indicates a pronounced synergistic effect between MWCNTs and specific plasticizing agents in enhancing the overall performance of SMA-16 compositions:

a) compositions 4 and 6, containing both MWCNTs and advanced plasticizers (selective extract and III vacuum fraction, respectively), demonstrated the highest GEC values (2.31 and 2.45), suggesting a well-balanced and superior multi-property performance (Fig. 7).

b) improvement in criteria such as rutting resistance (PQC_6), compressive strength at elevated temperatures (PQC_8), and long-term moisture resistance (PQC_5) was especially significant in nanomodified samples compared to their counterparts without MWCNTs (e.g., Composition 2 vs. 1, 4 vs. 3, and 6 vs. 5).

c) nanotube-free compositions consistently showed lower GEC values, confirming that the addition of MWCNTs contributes not only to individual property enhancements but also to overall structural efficiency.

The radar chart (Fig. 7) was constructed using the calculated values of Partial Quality Criteria (PQC1–PQC10) for six SMA-16 compositions (No. 1 to No. 6). It provides a visual comparison of the performance profiles of each composition across multiple quality dimensions. This graphical representation facilitates the identification of formulations with the most balanced and enhanced performance characteristics.

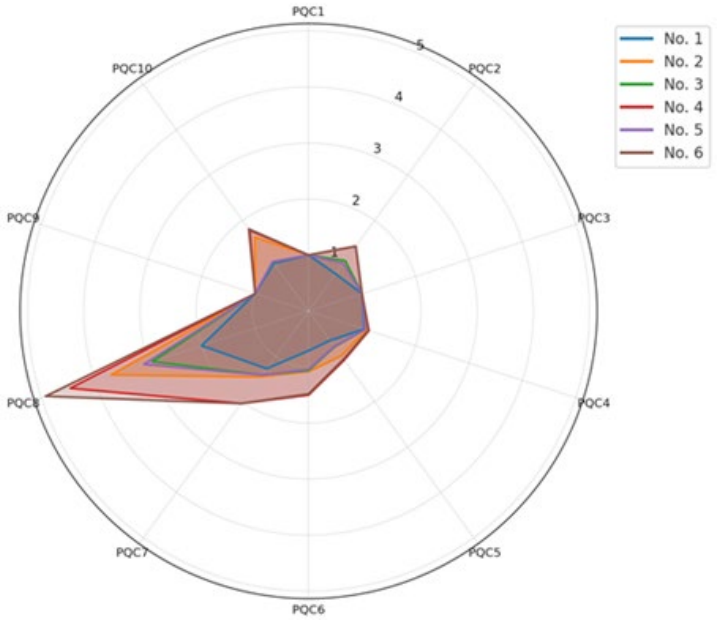

Fig. 7. Radar chart of PQC values for SMA-16 composition.

4. CONCLUSIONS

This study demonstrates that the incorporation of multi-walled carbon nanotubes (MWCNTs) into polymer-modified binders (PMBs) significantly improves their thermo-oxidative stability. Kinetic modeling using the Arrhenius equation revealed that MWCNT-modified binders exhibit a substantial reduction in the degradation rate constant and frequency factor, indicating suppressed molecular mobility and increased structural rigidity of the SBS network. The synergistic effect of MWCNTs with hydrocarbon plasticizers—specifically vacuum distillates and selective oil refining extracts—further enhances binder stability without negatively impacting key mixture parameters such as density and air void content in stone mastic asphalt (SMA).

Performance testing confirmed the enhanced durability of SMA mixtures containing MWCNT-based nanostructured systems, with marked improvements in water resistance, shear adhesion at elevated temperatures, and resistance to rutting under cyclic loading. Moreover, these modifications effectively mitigated strength loss after long-term freeze–thaw conditioning, confirming the protective role of MWCNTs at the binder–aggregate interface.

In addition to traditional testing metrics, a multi-criteria optimization methodology was applied to systematically evaluate the performance of stone mastic asphalt concrete. Ten normalized Partial Quality Criteria (PQC) were formulated, capturing key indicators of volumetric stability, water resistance, mechanical strength, and shear stability. These were integrated into a Generalized Effectiveness Coefficient (GEC), serving as a holistic index of functional performance. The nanomodified compositions, particularly those incorporating MWCNTs with SORE or VD carriers, demonstrated the highest GEC values, confirming their suitability for long-lasting pavement applications. This approach provides a robust analytical tool for comparing alternative formulations and optimizing mix design based on performance-driven objectives.

Future work will focus on field validation of the proposed nanomodified binders, along with long-term studies on fatigue resistance and aging behavior under real-world loading and climatic conditions.

5. ACKNOWLEDGEMENTS

The research was funded by the National Research Moscow State University of Civil Engineering (grant for fundamental scientific research, project No. 08-661/130)

REFERENCES

1. Shekhovtsova S.Y., Korolev E.V., Inozemtcev S.S., Yu J., Yu H. Method of forecasting the strength and thermal sensitive asphalt concrete. Magazine of Civil Engineering. 2019. 5. P. 129 – 140. DOI: 10.18720/MCE.89.11
2. Lyapin A.A., Parinov I.A., Buravchuk N.I., Cherpakov A.V., Shilyaeva O.V., Guryanova O.V. Improving Road Pavement Characteristics. Springer: Cham, Switzerland. 2020.
3. Tkach E., Shestakov N., Chertes K. Quality Assessment of Building Materials in the Construction of Bridge Structures. AIP Conference Proceedings. 2023. DOI: 10.1063/5.0143535
4. Guo M., Liang M., Jiao Y., Zhao W., Duan Y., Liu H. A review of phase change materials in asphalt binder and asphalt mixture. Construction and Building Materials. 2020. 258 (11). DOI:10.1016/j.conbuildmat.2020.119565
5. Tiwari N., Baldo N., Satyam N., Miani M. Mechanical characterization of industrial waste materials as mineral fillers in asphalt mixes: Integrated experimental and machine learning analysis. Sustainability. 2022. 14(10). P. 1 – 27. DOI:10.3390/su14105946
6. Bieliatynskyi A., Yang S., Pershakov V., Shao M., Ta M. Features of the structure and properties of stone mastic asphalt. Materialwissenschaft und Werkstofftechnik. 2024. 55 (7). P. 986 – 994. DOI:10.1002/mawe.202300181
7. Zheng Q., He P., Zhang D., Weng Y., Lu J., Wang T. A Holistic View of Asphalt Binder Aging under Ultraviolet Conditions: Chemical, Structural, and Rheological Characterization. Buildings. 2024. 14 (10). DOI:10.3390/buildings14103276
8. Gallego J., Gulisano F., Contreras V., Páez A. Optimising heat and re-compaction energy in the thermomechanical treatment for the assisted healing of asphalt mixtures. Construction and Building Materials. 2021. 292 (10). DOI:10.1016/j.conbuildmat.2021.123431
9. Ghadi H., Ghollasimood A., Pakniyat H., Khansari H., Eskandari H. Improving the resistance of asphalt mixtures against fatigue cracking with an interlayer. Geosynthetics: Leading the Way to a Resilient Planet. 2023. P. 266 – 272. CRC Press.
10. Bellatrache Y., Ziyani L., Dony A., Taki M., Haddadi S. Effects of the addition of date palm fibers on the physical, rheological and thermal properties of bitumen. Construction and Building Materials. 2020. 239 (1). DOI:10.1016/j.conbuildmat.2019.117808
11. Jin X., Guo N., You Z., Wang L., Wen Y., Tan Y. Rheological properties and micro-characteristics of polyurethane composite modified asphalt. Construction and Building Materials. 2020. 234 (7). DOI:10.1016/j.conbuildmat.2019.117395
12. Findik F. Nanomaterials and their applications. Periodicals of Engineering and Natural Sciences. 2021. 9. P. 62 – 75.
13. Golestani B., Nam B.H., Nejad F.M., Fallah S. Nanoclay application to asphalt concrete: Characterization of polymer and linear nanocomposite-modified asphalt binder and mixture. Construction and Building Materials. 2015. 91. P. 32 – 38. DOI:10.1016/j.conbuildmat.2015.05.019
14. Zhang H.L., Su M.M., Zhao S.F., Zhang Y.P., Zhang Z.P. High and low temperature properties of nano-particles/polymer modified asphalt. Construction and Building Materials. 2016. 114(1). P. 323 – 332. DOI:10.1016/j.conbuildmat.2016.03.118
15. Zhang H., Duan H., Zhu C., Chen Z., Luo H. Mini-review on the application of nanomaterials in improving anti-aging properties of asphalt. Energy Fuels 2021. 35 (14). DOI:10.1021/acs.energyfuels.1c01035
16. Obukhova S., Korolev E., Gladkikh V. The Influence of Single-Walled Carbon Nanotubes on the Aging Performance of Polymer-Modified Binders. Materials. 2023. 16 (24). DOI:10.3390/ma16247534

17. Eisa M.S., Mohamady A., Basiouny M.E., Abdulhamid A., Kim J.R. Mechanical properties of asphalt concrete modified with carbon nanotubes (CNTs). Case Studies in Construction Materials. 2022. 16 (4). DOI:10.1016/j.cscm.2022.e00930
18. Babagoli R. Laboratory investigation of the performance of binders and asphalt mixtures modified by carbon nano tube, poly phosphoric acid, and styrene butadiene rubber. Construction and Building Materials. 2021. 275 (1). DOI:10.1016/j.conbuildmat.2020.122178
19. de Melo J.V.S., Trichês G., de Rosso L.T. Experimental evaluation of the influence of reinforcement with Multi-Walled Carbon Nanotubes (MWCNTs) on the properties and fatigue life of hot mix asphalt Construction and Building Materials. 2018. 162. P. 369 – 382.
20. Xu J., Zhang A., Zhou T., Cao X., Xie Zh. A study on thermal oxidation mechanism of styrene–butadiene–styrene block copolymer (SBS). Polymer Degradation and Stability. 2007. 92 (9). P. 1682 – 1691.
21. Galano A. Carbon Nanotubes as Free-Radical Scavengers. The Journal of Physical Chemistry C. 2008. 112 (24). P. 8922 – 8927.
22. Martínez-Morlanes M.J., Castell P., Alonso P.J., Martinez M.T., Puértolas J.A. Multi-walled carbon nanotubes acting as free radical scavengers in gamma-irradiated ultrahigh molecular weight polyethylene composites. Carbon. 2012. 50 (7). P. 2442 – 2452.
23. Shi X., Jiang B., Wang J., Yang Y. Influence of wall number and surface functionalization of carbon nanotubes on their antioxidant behavior in high density polyethylene. Carbon. 2012. 50(3). P. 1005 – 1013.
24. Sai T., Ran S., Guo Z., Song P., Fang Z. Recent advances in fire-retardant carbon-based polymeric nanocomposites through fighting free radicals. SusMat. 2022. 2 (4). P. 411 – 434.
25. Xu X., You Y., Liu X., Wei D., Guan Y., Zheng A. Experimental and density functional theory investigations on the antioxidant mechanism of carbon nanotubes. Carbon. 2021. 177. P. 189 – 198.
26. Jambhulkar S., Ravichandran D., Zhu Y., Thippanna V., Ramanathan A., Patil D., Song K. Nanoparticle Assembly: From Self-Organization to Controlled Micropatterning for Enhanced Functionalities. Small 2024. 20 (6). DOI:10.1002/smll.202306394
27. Laidler K.J. The development of the Arrhenius equation. Journal of Chemical Education. 1984. 61 (6). P. 494.
28. Atkins P., De Paula J., Friedman R. Physical chemistry: quanta, matter, and change. Oxford University Press. 2014.
29. Wang Y., Sun L., Qin Y. Aging mechanism of SBS modified asphalt based on chemical reaction kinetics. Construction and Building Materials. 2015. 91. P. 47 – 56.
30. Cong P., Wang J., Luo W., Zhang Y. Effects of aging on the properties of SBS modified asphalt binders containing anti-aging agents. Construction and Building Materials. 2021. 302 (14-15). DOI:10.1016/j.conbuildmat.2021.124413
31. Lu X., Isacsson U. Effect of ageing on bitumen chemistry and rheology. Construction and Building Materials. 2002. 16(1). P. 15 – 22.
32. Wang R., Yue M., Xiong Y., Yue J. Experimental study on mechanism, aging, rheology and fatigue performance of carbon nanomaterial/SBS-modified asphalt binders. Construction and Building Materials. 2021. 268. DOI:10.1016/j.conbuildmat.2020.121189
33. Wang H., Yang J., Gong M. Rheological characterization of asphalt binders and mixtures modified with carbon nanotubes. In 8th RILEM International Symposium on Testing and Characterization of Sustainable and Innovative Bituminous Materials. 2016. P. 141 – 150.
34. Arifuzzaman M., Tarefder R.A., Islam M.S. The behavior of carbon nanotubes (CNTs) as a modifier to resist aging and moisture damage in asphalt. Nanoscience & Nanotechnology-Asia. 2021. 11(2). P. 224 – 229.
35. Ashish P.K., Singh D. Effect of Carbon Nano Tube on performance of asphalt binder under creep-recovery and sustained loading conditions. Construction and Building Materials. 2019. 215. P. 523 – 543.

INFORMATION ABOUT THE AUTHORS

Obukhova S.Yu., e-mail: shehovtsovasyu@mgsu.ru, ORCID ID: https://orcid.org/0000-0003-4490-0871, SCOPUS: https://www.scopus.com/authid/detail.uri?authorId=58258707000, Department of Urban Planning, Institute of Architecture and Urban Planning, National Research Moscow State University of Civil Engineering

Gladkikh V.A., e-mail: gladkich_87@mail.ru, ORCID ID: https://orcid.org/0000-0003-1953-1584, SCOPUS: https://www.scopus.com/authid/detail.uri?authorId=56432551500, Department of Urban Planning, Institute of Architecture and Urban Planning, National Research Moscow State University of Civil Engineering

Kuzmina T.K., e-mail: kuzminatk@mgsu.ru, ORCID ID: https://orcid.org/0000-0002-8454-1765, SCOPUS: https://www.scopus.com/authid/detail.uri?authorId=57192382306, Department of Technology and Organization of Construction Production, National Research Moscow State, University of Civil Engineering